The Linear Sampling Method in a waveguide : a modal formulation

L Bourgeois, E Lunéville

Laboratoire POEMS, UMR ENSTA‡/CNRS/INRIA, Ecole Nationale Supérieure des Techniques Avancées, 32 Boulevard Victor, 75739 Paris Cedex 15, France

Abstract. This paper concerns the Linear Sampling Method to retrieve obstacles in a 2D or 3D acoustic waveguide. The classical mathematical results concerning the identifiability of the obstacle and the justification of the inverse method are established for this particular geometry. Our main concern is to derive a modal formulation of the Linear Sampling Method that is well adapted to the waveguide configuration. In particular, thank's to such formulation, we highlight the fact that finding some obstacles from remote scattering data is more delicate in a waveguide than in free space. Indeed, the presence of evanescent modes increases the ill-posedness of the inverse problem. However, we show that numerical reconstruction of obstacles by using the far field is feasible, even by using a few incident waves.

1. Introduction

Since the introduction of the Linear Sampling Method by D. Colton and A. Kirsch [7], a considerable amount of papers have concerned this new method for solving inverse diffraction problems in acoustics. The main attractive feature of such method is it does not require *a priori* knowledge about the boundary condition on the boundary of the unknown scatterer. The book [5] and the review paper [6] present a great number of situations in which we can apply the LSM.

However, it seems to the authors that very few papers concern the Linear Sampling Method in a waveguide. It is well known that imaging a scatterer in a waveguide is much more challenging than in free space. Indeed, because of the presence of the boundary of the waveguide, only a finite number of modes can propagate at long distance, while the other modes decay exponentially as a function of distance. This phenomenon considerably increases the ill-posedness of the inverse problem.

Some authors have explored this issue. In [17], the LSM is used to image an obstacle in a 2D shallow ocean with near field, precisely with data on a top horizontal straight line. In [3], the technique of the convex scattering support [16], which has some connections with the LSM, is used to image an obstacle in a 3D shallow ocean with the help of the far field. The authors of [1] use the factorization method [12], which can be considered

‡ member of ParisTech

as a refined version of the LSM, to recover the scattering surface of a periodic structure. Finally, in [10], the authors use what they call the "eigensystem decomposition" and the Lippman-Schwinger equation to recover inhomogeneities in a 2D waveguide. However, only small inhomogeneities are considered in their paper since the Born approximation is used.

The following paper concerns the Linear Sampling Method in a 2D or 3D acoustic waveguide and presents a modal formulation of the method. The aim of such formulation is to highlight the specific properties of the waveguide modes we have described before, and to understand how to adapt the numerical strategy to take these specific properties into account. This seems necessary in particular when, as in our paper, the support of data is a section of the waveguide which is far away from the obstacle, contrary to the problem solved in [17]. In other words, our main concern is to answer the following question : is it possible to recover unknown scatterers by using the far field ? From a practical point of view, for example in the field of non destructive evaluation, this seems an interesting point to consider.

The paper is organized as follows. In section 2, we recall some basic properties of the forward problem. In section 3, we analyze the Green function in the waveguide, as well as the scattered field which is associated to an incident wave which consists of such Green function. In section 4, we introduce the inverse problem we consider and show how the LSM applies to it. In particular, we offer a uniqueness theorem, as well as a mathematical justification for the LSM, by simply adapting to the waveguide configuration the framework of [15, 4], introduced in the case of free space. In section 5, we describe our modal analysis of the LSM. Lastly, numerical results in 2D are presented in section 6.

2. The forward problem

We consider a waveguide of domain $W = \mathbb{R} \times \Sigma$ in $\mathbb{R}^d$ with $d = 2$ or $d = 3$. In 2D, $\Sigma = (0, h)$, where $h > 0$, while in 3D, Σ is a bounded and open domain of $\mathbb{R}^2$, the boundary of which is C^∞ and denoted Γ. In the following, $x(x_1, x_2)$ will denote a generic point of W, where $x_1 \in \mathbb{R}$ and $x_2 \in \Sigma$.

It is well known that the solutions of the Neumann eigenvalue problem for the negative Laplacien in Σ form an increasing sequence $k_n^2 \in \mathbb{R}^+$ for $n \in \mathbb{N}$, with $k_0 = 0$ and $k_n \to +\infty$ when $n \to +\infty$, and that we can find some eigenvectors θ_n which form an orthonormal basis of $L^2(\Sigma)$.

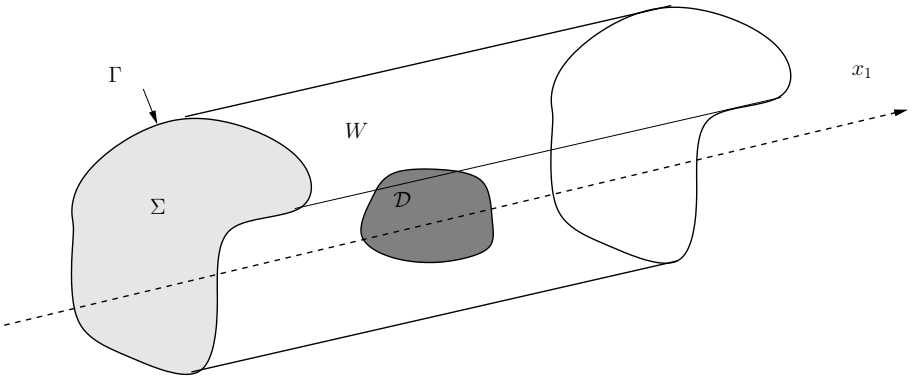

The solutions of the problem

$$\begin{cases} (\Delta + k^2)u = 0 & \text{in} \quad W \\ \partial_\nu u = 0 & \text{on} \quad \Gamma, \end{cases} \tag{1}$$

where ν is the outward unit normal on Γ, are the linear combinations of the functions defined for $n \in \mathbb{N}$ by

$$g_n^\pm(x_1, x_2) = \theta_n(x_2) e^{\pm i\beta_n x_1}, \quad \beta_n = \sqrt{k^2 - k_n^2}, \quad \mathrm{Re}\,\beta_n, \mathrm{Im}\,\beta_n \geq 0, \tag{2}$$

as can be seen at the beginning of the proof of lemma 1 (see appendix A).

Remark : in 2D, for example, we have

$$\beta_n = \sqrt{k^2 - \left(\frac{n\pi}{h}\right)^2}, \quad \begin{cases} \theta_0(x_2) = \sqrt{\frac{1}{h}} \\ \theta_n(x_2) = \sqrt{\frac{2}{h}} \cos(\frac{n\pi}{h} x_2) \quad (n \geq 1). \end{cases}$$

In the following, we assume that $\beta_n \neq 0$ for all $n \geq 0$. Functions $g_n^\pm$ are called the guided modes of the waveguide. There is a finite number N_p such that the N_p first β_n have $\mathrm{Re}\,\beta_n > 0$, the rest of the β_n having $\mathrm{Im}\,\beta_n > 0$. Consequently, the N_p first guided modes g_n^+ (respectively g_n^-) are propagating from the left to the right of the waveguide (respectively from the right to the left), while the other guided modes g_n^+ (respectively g_n^-) are decaying exponentially from the left to the right of the waveguide (respectively from the right to the left).

We define now $\Sigma_s = \{s\} \times \Sigma$. Let $\mathcal{D}$ be an open bounded domain within W, the boundary of which is Lipschitz continuous and denoted ∂D. This obstacle is assumed to lie between sections Σ_{-t_0} and Σ_{t_0}, with $t_0 > 0$.
For $k > 0$ and $f \in H^{1/2}(\partial\mathcal{D})$, the forward problem we consider is

$$\begin{cases} (\Delta + k^2)u = 0 & \text{in} \quad W \setminus \overline{\mathcal{D}} \\ \partial_\nu u = 0 & \text{on} \quad \Gamma \\ u = f & \text{on} \quad \partial\mathcal{D} \\ \partial_\nu u = T^\pm u & \text{on} \quad \Sigma_{\pm t}. \end{cases} \tag{3}$$

Here, $t > t_0$ and $T^\pm$ is the Dirichlet to Neumann operator $T^\pm : H^{1/2}(\Sigma_{\pm t}) \longrightarrow H^{-1/2}(\Sigma_{\pm t})$, defined for $h \in H^{1/2}(\Sigma_{\pm t})$ by

$$T^\pm h = \sum_{n \in \mathbb{N}} i\beta_n (h, \theta_n)_{\Sigma_{\pm t}} \theta_n,$$

where $(.,.)_{\Sigma_s}$ is the standard scalar product in $L^2(\Sigma_s)$.
The solution u of problem (3) is the scattered field due to the soft obstacle $\mathcal{D}$, where the data $-f$ is the trace on $\partial\mathcal{D}$ of an incident wave, which in the following will be either the Green function G or a guided mode $g_n^{\pm}$ of the waveguide. The last condition in problem (3) is a radiation condition. It consists of assuming that the scattered field u is a superposition of guided modes that are outgoing, that is either propagating away from the obstacle or decaying exponentially with distance from the obstacle. It is well-known (see for example [2]) that for a given obstacle $\mathcal{D}$ the problem (3) is well-posed in $H^1_{loc}(W \setminus \overline{\mathcal{D}})$, except for at most a countable set of wavenumbers k. Hence we introduce the following assumption, which is supposed to hold throughout this paper.

Assumption (H_0) *: k is such that problem (3) is well-posed.*

The following lemma (see appendix A for the proof) will be very useful in the following.

Lemma 1 *For all $s < t$ and $h \in H^{1/2}(\Sigma_s)$, the following problem without the obstacle*

$$\begin{cases} (\Delta + k^2)u = 0 & in \quad (s,t) \times \Sigma \\ \partial_\nu u = 0 & on \quad (s,t) \times \partial\Sigma \\ u = h & on \quad \Sigma_s \\ \partial_\nu u = T^+ u & on \quad \Sigma_t \end{cases}$$

has a unique solution in $H^1((s,t) \times \Sigma)$, which is given by

$$u(x_1, x_2) = \sum_{n \in \mathbb{N}} (h, \theta_n)_{\Sigma_s} e^{i\beta_n(x_1 - s)} \theta_n(x_2).$$

Of course, a similar lemma may be claimed in the domain $(-t, s) \times \Sigma$ for $s > -t$ with radiation condition $\partial_\nu u = T^- u$ on Σ_{-t}.

3. The Green function and the associated scattered field

For a given point $y(y_1, y_2) \in W$, we denote by $G(x, y)$ the solution of problem

$$\begin{cases} (\Delta_x + k^2)G(., y) = \delta_y & \text{in} \quad W \\ \partial_{\nu_x} G(., y) = 0 & \text{on} \quad \Gamma \\ \partial_{\nu_x} G(., y) = T^{\pm} G(., y) & \text{on} \quad \Sigma_{\pm t}, \end{cases}$$

that is the Green function of the waveguide W. The function G is defined, for all $x, y \in W$, by

$$G(x, y) = \sum_{n \in \mathbb{N}} \frac{e^{i\beta_n |x_1 - y_1|}}{2i\beta_n} \theta_n(x_2)\theta_n(y_2). \tag{4}$$

This expansion results for example from a classical technique which uses the limiting absorption principle, that is k is replaced by $k + i\varepsilon$ with $\varepsilon > 0$, then the Fourier transform along the x_1 direction in order to solve the problem in the transverse section Σ, a residue theorem in order to come back to variable x_1, and lastly the passage to the limit $\varepsilon \to 0$.

Clearly, if $\Phi(x,y)$ is the Green function of the Helmholtz equation in $\mathbb{R}^d$, $G(.,y)-\Phi(.,y)$ is a C^∞ function in $\overline{W}$, and hence $G(.,y)$ is smooth except in a vicinity of $x=y$, where it behaves as the function $\Phi(.,y)$. To be more precise, we have in 2D,

$$G(x,y) \sim \frac{1}{2i} H_0^1(k(||x-y||)) \sim \frac{1}{2\pi} \log(k||x-y||) \quad \text{when} \quad x \to y,$$

and in 3D,

$$G(x,y) \sim -\frac{e^{ik(||x-y||)}}{4\pi||x-y||} \quad \text{when} \quad x \to y.$$

In particular $G(.,y) \notin H^1_{loc}(W)$ in both cases, which is an important thing to note in the following.
We denote by $u^s(.,y)$ the solution of the problem (3) with $f=-G(.,y)|_{\partial\mathcal{D}}$, $y \notin \partial\mathcal{D}$.
We will need the two following lemmas (see appendices B and C for the proofs).

Lemma 2 (integral representation) *Let u be the solution of (3) for a $f \in H^{1/2}(\partial\mathcal{D})$. For all $x \in W \setminus \overline{\mathcal{D}}$, we have the representation formula*

$$u(x) = \int_{\partial\mathcal{D}} \left(u(y) \frac{\partial G(x,y)}{\partial \nu_y} - \frac{\partial u(y)}{\partial \nu_y} G(x,y) \right) ds(y),$$

where ν_y is the unit normal oriented to the exterior of $W \setminus \overline{\mathcal{D}}$.

Lemma 3 (reciprocity)

$$\forall x, y \in W \setminus \overline{\mathcal{D}}, \quad u^s(x,y) = u^s(y,x).$$

4. The inverse problem and the Linear Sampling Method

4.1. Objective

We assume that we impose an incident wave of form $G(.,y)$ for $y \in \hat{\Sigma}$, and we measure the corresponding scattered field $u^s(x,y)$ due to the obstacle $\mathcal{D}$ for $x \in \hat{\Sigma}$. As far as the definition of $\hat{\Sigma}$ is concerned, we will consider the following situations :

(1) $\hat{\Sigma} = \Sigma_{-s} \cup \Sigma_s$

(2) $\hat{\Sigma} = \Sigma_s$

for some $s > t_0$. The case (1) will be called the full aperture situation, while the case (2) will be called the back-scattering situation.
In the two cases, the objective is to determine $\mathcal{D}$ from the measurements of $u^s(.,y)$ on $\hat{\Sigma}$ for all $y \in \hat{\Sigma}$.
In the following, the results hold for both situations (1) and (2).

4.2. The near field operator and its factorization

We first introduce the following assumption.

Assumption (H) *: k^2 is not a Dirichlet eigenvalue for the negative Laplacian in $\mathcal{D}$.*

Secondly, we introduce the same type of operators as in [4] with similar notations. Let us define the near field operator $F : L^2(\hat{\Sigma}) \to L^2(\hat{\Sigma})$ such that for $h \in L^2(\hat{\Sigma})$,

$$(Fh)(x) = \int_{\hat{\Sigma}} u^s(x,y)h(y)\,ds(y), \quad x \in \hat{\Sigma}, \tag{5}$$

the operator $B : H^{1/2}(\partial\mathcal{D}) \to L^2(\hat{\Sigma})$ such that for $f \in H^{1/2}(\partial\mathcal{D})$, $Bf = u|_{\hat{\Sigma}}$, where u is the solution of problem (3). Next, we define $\mathcal{H} : L^2(\hat{\Sigma}) \to H^{1/2}(\partial\mathcal{D})$ such that for $h \in L^2(\hat{\Sigma})$, $\mathcal{H}h = v_h|_{\partial\mathcal{D}}$, where v_h is the function defined by

$$v_h(x) = \int_{\hat{\Sigma}} G(x,y)h(y)\,ds(y). \tag{6}$$

Lastly, we define $\mathcal{F} : H^{-1/2}(\partial\mathcal{D}) \to L^2(\hat{\Sigma})$ by

$$(\mathcal{F}\phi)(x) = \int_{\partial\mathcal{D}} \phi(y)G(x,y)\,ds(y), \quad x \in \hat{\Sigma}$$

and $S : H^{-1/2}(\partial\mathcal{D}) \to H^{1/2}(\partial\mathcal{D})$ by

$$(S\phi)(x) = \int_{\partial\mathcal{D}} \phi(y)G(x,y)\,ds(y), \quad x \in \partial\mathcal{D}.$$

The two above integrals have the sense of duality pairing between $H^{-1/2}(\partial\mathcal{D})$ and $H^{1/2}(\partial\mathcal{D})$.

The following proposition is of major importance.

Proposition 1 *S is an isomorphism if assumption (H) is satisfied.*

Proof : the result is well-known when the kernel $G(x,y)$ of the waveguide is replaced by the kernel $\Phi(x,y)$, which is the Green function of the Helmholtz equation in $\mathbb{R}^d$. This remark will enable us to prove this proposition. We decompose

$$G(x,y) = \Phi(x,y) + R(x,y),$$

and we define $S_0 : H^{-1/2}(\partial\mathcal{D}) \to H^{1/2}(\partial\mathcal{D})$ by

$$(S_0\phi)(x) = \int_{\partial\mathcal{D}} \phi(y)\Phi(x,y)\,ds(y), \quad x \in \partial\mathcal{D}.$$

Since the kernel of $S - S_0$ is the smooth function $R(x,y)$, it is clear that $(S - S_0)(\phi)$ is a C^∞ function on $\overline{W}$ and that $S - S_0$ is continuous. First, the fact that $S\phi \in H^{1/2}(\partial\mathcal{D})$ and that S is continuous result from the same properties for S_0.

Next, let us consider injectivity and suppose $S\phi = 0$ on $\partial\mathcal{D}$. Let us denote $\mathcal{S}$ and $\mathcal{S}_0$, the single-layer potentials with kernels $G(x,y)$ and $\Phi(x,y)$ respectively. We know that $\mathcal{S}_0\phi \in H^1_{loc}(\mathbb{R}^d)$ ($d = 2$ or $d = 3$) defines two functions u_0^- and u_0^+ in $\mathcal{D}$ and $\mathbb{R}^d \setminus \overline{\mathcal{D}}$ respectively, with $u_0^+|_{\partial\mathcal{D}} = u_0^-|_{\partial\mathcal{D}} = S_0\phi$. It implies that $\mathcal{S}\phi \in H^1_{loc}(W)$ defines two functions u^- and u^+ in $\mathcal{D}$ and $W \setminus \overline{\mathcal{D}}$ respectively, with $u^+|_{\partial\mathcal{D}} = u^-|_{\partial\mathcal{D}} = S\phi = 0$. From

uniqueness of Dirichlet problems in $\mathcal{D}$ (thank's to assumption H) and $W \setminus \overline{\mathcal{D}}$ (thank's to assumption H_0), we obtain $u^- = u^+ = 0$ and then $(\partial u^+/\partial\nu)|_{\partial\mathcal{D}} = (\partial u^-/\partial\nu)|_{\partial\mathcal{D}} = 0$, where ν is the outward unit normal outside $\mathcal{D}$. To complete the proof of injectivity, we know that

$$\phi = \left(\frac{\partial u_0^+}{\partial\nu} - \frac{\partial u_0^-}{\partial\nu}\right)|_{\partial\mathcal{D}} = \left(\frac{\partial u^+}{\partial\nu} - \frac{\partial u^-}{\partial\nu}\right)|_{\partial\mathcal{D}} = 0.$$

Lastly, we prove surjectivity. Let $f \in H^{1/2}(\partial\mathcal{D})$, u^- and u^+ the solutions of Helmholtz problems in $\mathcal{D}$ and $W \setminus \overline{\mathcal{D}}$ which corresponds to the Dirichlet data f (these problems are well-posed, see [2]). We denote

$$\phi = \left(\frac{\partial u^+}{\partial\nu} - \frac{\partial u^-}{\partial\nu}\right)|_{\partial\mathcal{D}},$$

$$w(x) := \int_{\partial\mathcal{D}} \phi(y) G(x,y)\, dy,$$

and the corresponding functions w^- and w^+ in $\mathcal{D}$ and $W \setminus \overline{\mathcal{D}}$. The functions w^- and w^+ satisfy $(w^+ - w^-)|_{\partial\mathcal{D}} = 0$ and $(\partial w^+/\partial\nu)|_{\partial\mathcal{D}} - (\partial w^-/\partial\nu)|_{\partial\mathcal{D}} = \phi$. The functions u^- and u^+ satisfy the same relationships at boundary $\partial\mathcal{D}$, so that $u - w$ satisfies problem (1) and is consequently a linear combination of the functions $g_n^\pm$ defined by (2). Since it satisfies the radiation condition too, this linear combination necessarily vanishes, and $u = w$ in W. We hence obtain $f = S\phi$, which completes the proof. ■

Like in [4], factorization of operator F helps to simplify the following analysis. By superposition, we straightforward obtain the relationships

$$F = -B\mathcal{H} \tag{7}$$

and

$$\mathcal{F} = BS, \tag{8}$$

and then, because S is an isomorphism, we obtain the factorization

$$F = -\mathcal{F}S^{-1}\mathcal{H}. \tag{9}$$

The operators $\mathcal{H}$, $\mathcal{F}$ and F satisfy the following properties.

Proposition 2 *$\mathcal{H}$, $\mathcal{F}$ and F are compact operators ; they are injective with dense range if assumption (H) is satisfied.*

Proof : the proof is detailed only in the back-scattering case, the proof in the full aperture case would need a very slight adaptation. We begin with operator $\mathcal{H}$. Since its kernel $G(x,y)$ is $C^\infty(\partial\mathcal{D} \times \overline{\Sigma_s})$, $\mathcal{H}$ is compact (see [13], p. 20).
Concerning injectivity, if $h \in L^2(\Sigma_s)$ satisfies

$$v_h(x) = \int_{\Sigma_s} G(x,y) h(y)\, ds(y) = 0 \quad \text{on} \quad \partial\mathcal{D},$$

v_h is a function that solves the Helmholtz equation in $\mathcal{D}$ and vanishes on $\partial\mathcal{D}$. Because of assumption (H), v_h vanishes in domain $\mathcal{D}$ and then in W with the help of the

unique continuation theorem. In particular, $v_h|_{\Sigma_s} = 0$ and by using formula (4) and a decomposition $h = \sum_{n\in\mathbb{N}} h_n\theta_n$, we obtain

$$\sum_{n\in\mathbb{N}} \frac{1}{2i\beta_n} h_n\theta_n = 0 \quad \text{on} \quad \Sigma_s,$$

and then $h_n = 0$ for all $n \geq 0$, that is $\mathcal{H}$ is injective.
To show that $\mathcal{H}$ has dense range, we have to prove that its adjoint $\mathcal{H}^* : H^{-1/2}(\partial\mathcal{D}) \to L^2(\Sigma_s)$ is injective. We have for $\phi \in H^{-1/2}(\partial\mathcal{D})$ and $h \in L^2(\Sigma_s)$,

$$\left\langle \phi, \int_{\Sigma_s} G(.,y)h(y)\, ds(y) \right\rangle_{H^{-1/2}(\partial\mathcal{D}),H^{1/2}(\partial\mathcal{D})} = \int_{\Sigma_s} \overline{h(y)}\, \langle \phi, G(.,y)\rangle_{H^{-1/2}(\partial\mathcal{D}),H^{1/2}(\partial\mathcal{D})}\, ds(y).$$

This result is a consequence of the Fubini's theorem when $\phi \in L^2(\partial\mathcal{D})$, which is not the case here. But the result remains true for $\phi \in H^{-1/2}(\partial\mathcal{D})$ since for a Lipschitz continuous domain $\mathcal{D}$, $L^2(\partial\mathcal{D})$ is dense in $H^{-1/2}(\partial\mathcal{D})$. As a result, and using the fact that $G(x,y) = G(y,x)$, $\mathcal{H}^*$ is defined by

$$(\mathcal{H}^*\phi)(x) = \langle \phi(y), G(x,y)\rangle, \quad x \in \Sigma_s.$$

Using the decomposition formula (4), we have for $x_1 > s$,

$$\langle \phi(y), G(x,y)\rangle = \sum_{n\in\mathbb{N}} \frac{\overline{e^{i\beta_n x_1}}}{2i\beta_n}\theta_n(x_2) < \phi(y), e^{-i\beta_n y_1}\theta_n(y_2) > .$$

If $\mathcal{H}^*\phi$ vanishes on Σ_s, then we have that $< \phi(y), e^{-i\beta_n y_1}\theta_n(y_2) >= 0$ for all $n \geq 0$, which implies $\langle \phi(y), G(x,y)\rangle = 0$ for $x_1 > s$, and then $\langle \phi(y), G(x,y)\rangle = 0$ for all $x \in W \setminus \overline{\mathcal{D}}$ by using the unique continuation theorem, and finally on $\partial\mathcal{D}$ as well, with the help of the trace theorem. We complete the proof of injectivity of $\mathcal{H}^*$ by using the injectivity of operator S.
As concerns $\mathcal{F}$, we remark that

$$\mathcal{F}\phi = \overline{\mathcal{H}^*}\phi := \overline{\mathcal{H}^*\overline{\phi}},$$

which proves that $\mathcal{F}$ is compact, injective with dense range. The same properties hold for F by using equation (9). ■

4.3. A uniqueness result

We first verify that the measurements of $u^s(.,y)$ on $\hat{\Sigma}$ for all $y \in \hat{\Sigma}$ uniquely determine the soft obstacle $\mathcal{D}$.

Theorem 1 *Let us denote by $\mathcal{D}_1$ and $\mathcal{D}_2$ two soft obstacles whose boundaries are Lipschitz continuous. If we assume that for all incident waves $G(.,y)$ with $y \in \hat{\Sigma}$, the corresponding scattered fields $u_1^s(.,y)$ and $u_2^s(.,y)$ coincide on $\hat{\Sigma}$, then $\mathcal{D}_1 = \mathcal{D}_2$.*

Since the proof is the same as in [15], p. 122, it is not repeated here. In the case of the waveguide, it is based on the reciprocity relationship given by lemma 3.

4.4. Mathematical basis of the LSM

The Linear Sampling Method is based on the following equation : find $h(.,z) \in L^2(\hat{\Sigma})$ such that

$$Fh = G(.,z), \tag{10}$$

where z is a sampling point of W. The method consists in finding a quasi-solution of (10) for each z and then in plotting the norm of $h(.,z)$, which happens to explode outside the obstacle $\mathcal{D}$. This method is justified in part by the following theorem, which is very similar as the one presented in [4]. For that reason, the proof of the theorem, which is mainly based on proposition 2, is omitted.

Theorem 2 *We assume that (H) is satisfied for an obstacle $\mathcal{D}$ with Lipschitz continuous boundary. Let F be the near field operator defined by (5) with $u^s(.,y)$ being the solution of problem (3) with $f = -G(.,y)|_{\partial\mathcal{D}}$.*
(1) If $z \in \mathcal{D}$, then for all $\varepsilon > 0$ there exists a solution $h_\varepsilon(.,z) \in L^2(\hat{\Sigma})$ of the inequality

$$||Fh_\varepsilon(.,z) - G(.,z)||_{L^2(\hat{\Sigma})} \leq \varepsilon$$

such that the function $\mathcal{H}h_\varepsilon(.,z)$ converges in $H^{1/2}(\partial D)$ as $\varepsilon \to 0$.
Furthermore, for a given fixed ε, the function $h_\varepsilon(.,z)$ satisfies

$$\lim_{z\to\partial\mathcal{D}} ||h_\varepsilon(.,z)||_{L^2(\hat{\Sigma})} = \infty, \quad \lim_{z\to\partial\mathcal{D}} ||\mathcal{H}h_\varepsilon(.,z)||_{H^{1/2}(\partial D)} = \infty.$$

(2) If $z \in W \setminus \overline{\mathcal{D}}$, then every solution $h_\varepsilon(.,z) \in L^2(\hat{\Sigma})$ of the inequality

$$||Fh_\varepsilon(.,z) - G(.,z)||_{L^2(\hat{\Sigma})} \leq \varepsilon$$

satisfies

$$\lim_{\varepsilon\to 0} ||h_\varepsilon(.,z)||_{L^2(\hat{\Sigma})} = \infty, \quad \lim_{\varepsilon\to 0} ||\mathcal{H}h_\varepsilon(.,z)||_{H^{1/2}(\partial D)} = \infty.$$

5. A modal analysis of the LSM

The aim of this section is to present a modal version of the Linear Sampling Method. It will be obtained by projecting the relationship (10) upon the functions θ_n, which form an orthonormal basis in $L^2(\Sigma)$. This is motivated by the particular form of the Green function of the waveguide (4) and the fact that far field contains only propagating modes.

5.1. Projection upon modes

We denote by $u_n^\pm$ the solution for $n \in \mathbb{N}$ of problem (3) with $f = -g_n^\pm|_{\partial\mathcal{D}}$. To begin with, we have to find an expression of u^s only in terms of the u_n^- and the u_n^+, which is the aim of the following proposition.

Proposition 3

$$\forall x \in W\backslash\overline{\mathcal{D}}, \quad u^s(x,y) = \begin{cases} \displaystyle\sum_{n\in\mathbb{N}} \frac{e^{i\beta_n|y_1|}}{2i\beta_n}\theta_n(y_2)u_n^-(x) \quad \text{if} \quad y_1 = s > t_0 \\ \displaystyle\sum_{n\in\mathbb{N}} \frac{e^{i\beta_n|y_1|}}{2i\beta_n}\theta_n(y_2)u_n^+(x) \quad \text{if} \quad y_1 = -s < -t_0. \end{cases} \tag{11}$$

Proof : we first assume that $y_1 = s > t_0$, and we denote

$$H(x,y) = \sum_{n\in\mathbb{N}} \frac{e^{i\beta_n|y_1|}}{2i\beta_n}\theta_n(y_2)u_n^-(x).$$

Since the solution of problem (3) with $f = -G(.,y)|_{\partial\mathcal{D}}$ is unique, we only have to prove that $H(.,y)$ solves such problem. The only non trivial thing to verify is that $H(.,y) = -G(.,y)$ on $\partial\mathcal{D}$. For $x \in \partial\mathcal{D}$ we have by using the definition of the u_n^-,

$$H(x,y) = -\sum_{n\in\mathbb{N}} \frac{e^{i\beta_n|y_1|}}{2i\beta_n}\theta_n(y_2)g_n^-(x)$$

$$= -\sum_{n\in\mathbb{N}} \frac{e^{i\beta_n y_1}}{2i\beta_n}e^{-i\beta_n x_1}\theta_n(x_2)\theta_n(y_2)$$

$$= -\sum_{n\in\mathbb{N}} \frac{e^{i\beta_n|x_1-y_1|}}{2i\beta_n}\theta_n(x_2)\theta_n(y_2),$$

since $x_1 < t_0 < y_1$, and finally $H(x,y) = -G(x,y)$. The proof is similar for $y_1 = -s < -t_0$. ■

Next we find the expression of F in terms of the θ_n. We do it in the full aperture situation, the decomposition of F in the back-scattering situation will automatically result from the first one. To this end, we assume that $h = (h^-, h^+) \in L^2(\Sigma_{-s}) \times L^2(\Sigma_s)$, the decomposition of h^- (resp. h^+) in terms of the θ_n being denoted h_n^- (resp. h_n^+). By using proposition 3 and definition (5), we have for $x \in \Sigma_{-s}$,

$$(Fh)(x) = \int_{\Sigma_{-s}} u^s(x,y)h^-(y)\,ds(y) + \int_{\Sigma_s} u^s(x,y)h^+(y)\,ds(y)$$

$$= \sum_{n\in\mathbb{N}} \int_{\Sigma_{-s}} \frac{e^{i\beta_n|y_1|}}{2i\beta_n}\theta_n(y_2)u_n^+(x)h^-(y)\,ds(y) + \sum_{n\in\mathbb{N}} \int_{\Sigma_s} \frac{e^{i\beta_n|y_1|}}{2i\beta_n}\theta_n(y_2)u_n^-(x)h^+(y)\,ds(y)$$

$$= \sum_{n\in\mathbb{N}} \frac{e^{i\beta_n s}}{2i\beta_n}\left(u_n^+(x)h_n^- + u_n^-(x)h_n^+\right).$$

Let us denote for $x \in \Sigma_{-s}$,

$$u_n^+(x) = \sum_{m\in\mathbb{N}} (U_n^+)_m^-\,\theta_m(x_2), \quad u_n^-(x) = \sum_{m\in\mathbb{N}} (U_n^-)_m^-\,\theta_m(x_2).$$

We obtain for $x \in \Sigma_{-s}$,

$$(Fh)(x) = \sum_{m\in\mathbb{N}}\sum_{n\in\mathbb{N}} \frac{e^{i\beta_n s}}{2i\beta_n}\left((U_n^+)_m^-\,h_n^- + (U_n^-)_m^-\,h_n^+\right)\theta_m(x_2).$$

Similarly, if we note for $x \in \Sigma_s$

$$u_n^+(x) = \sum_{m\in\mathbb{N}} (U_n^+)_m^+ \, \theta_m(x_2), \quad u_n^-(x) = \sum_{m\in\mathbb{N}} (U_n^-)_m^+ \, \theta_m(x_2),$$

we obtain that for $x \in \Sigma_s$,

$$(Fh)(x) = \sum_{m\in\mathbb{N}} \sum_{n\in\mathbb{N}} \frac{e^{i\beta_n s}}{2i\beta_n} \left((U_n^+)_m^+ \, h_n^- + (U_n^-)_m^+ \, h_n^+ \right) \theta_m(x_2).$$

From these two results we obtain the compacted formula : for $x \in \Sigma_{\pm s}$,

$$(Fh)(x) = \sum_{m\in\mathbb{N}} \sum_{n\in\mathbb{N}} \frac{e^{i\beta_n s}}{2i\beta_n} \left((U_n^+)_m^\pm \, h_n^- + (U_n^-)_m^\pm \, h_n^+ \right) \theta_m(x_2). \tag{12}$$

In the back-scattering situation, we have for $x \in \Sigma_s$,

$$(Fh)(x) = \sum_{m\in\mathbb{N}} \sum_{n\in\mathbb{N}} \frac{e^{i\beta_n s}}{2i\beta_n} (U_n^-)_m^+ \, h_n^+ \, \theta_m(x_2).$$

On the other hand, the right-hand side of (10) is, for $-s < -t_0 < z_1 < t_0 < s$,

$$G(x,z) = \sum_{m\in\mathbb{N}} \frac{e^{i\beta_m |x_1 - z_1|}}{2i\beta_m} \theta_m(x_2)\theta_m(z_2),$$

that is for $x \in \Sigma_{\pm s}$,

$$G(x,z) = \sum_{m\in\mathbb{N}} \frac{e^{i\beta_m (s \mp z_1)}}{2i\beta_m} \theta_m(z_2)\theta_m(x_2). \tag{13}$$

Gathering (12) and (13), the equation (10) in the full aperture situation is equivalent to

$$\forall m \in \mathbb{N}, \quad \begin{cases} \displaystyle\sum_{n\in\mathbb{N}} \frac{e^{i\beta_n s}}{i\beta_n} \left((U_n^+)_m^- \, h_n^- + (U_n^-)_m^- \, h_n^+ \right) = \frac{e^{i\beta_m (s+z_1)}}{i\beta_m} \theta_m(z_2) \\ \displaystyle\sum_{n\in\mathbb{N}} \frac{e^{i\beta_n s}}{i\beta_n} \left((U_n^+)_m^+ \, h_n^- + (U_n^-)_m^+ \, h_n^+ \right) = \frac{e^{i\beta_m (s-z_1)}}{i\beta_m} \theta_m(z_2). \end{cases} \tag{14}$$

In the back-scattering situation, the equation (10) is equivalent to

$$\forall m \in \mathbb{N}, \quad \sum_{n\in\mathbb{N}} \frac{e^{i\beta_n s}}{i\beta_n} (U_n^-)_m^+ \, h_n^+ = \frac{e^{i\beta_m (s-z_1)}}{i\beta_m} \theta_m(z_2). \tag{15}$$

One of the more important fact concerning the Linear Sampling Method in a waveguide is that, as the equations (14) and (15) show it :

(i) in the full aperture situation, measuring for $x \in \Sigma_{\pm s}$ the scattered fields $u^s(x,y)$ due to the incident waves of form $G(.,y)$ for $y \in \Sigma_{\pm s}$ is equivalent to measuring the projections on the θ_m of the scattered fields $u_n^\pm(x)$ for $x \in \Sigma_{\pm s}$, due to the incident waves $g_n^\pm$ for all $m, n \in \mathbb{N}$,

(ii) in the back-scattering situation, measuring for $x \in \Sigma_s$ the scattered fields $u^s(x,y)$ due to the incident waves of form $G(.,y)$ for $y \in \Sigma_s$ is equivalent to measuring the projections on the θ_m of the scattered fields $u_n^-(x)$ for $x \in \Sigma_s$, due to the incident waves g_n^- for all $m, n \in \mathbb{N}$.

5.2. Restriction to a finite number of modes

For numerical purpose, we have to restrict ourselves to a finite number M of indices m and a finite number N of indices n in equations (14) and (15), since we impose a finite number of incident modes, and we project the measurements of the corresponding scattered fields upon a finite number of transverse eigenfunctions. For simplicity, we assume that $M = N$, and that these N modes correspond to N_p propagating modes and N_e evanescent modes. Therefore, the equations (14) and (15) lead to a system

$$UH = C. \tag{16}$$

For example, in the back-scattering situation, the $N \times N$ matrix U and the N vectors H, C are defined respectively by

$$U_{mn} = \frac{e^{i\beta_n s}}{i\beta_n}(U_n^-)_m^+, \quad H_n = h_n^+, \quad C_m = \frac{e^{i\beta_m(s-z_1)}}{i\beta_m}\theta_m(z_2). \tag{17}$$

If we separate propagating and evanescent modes, (16) can be written as follows :

$$\begin{pmatrix} U^{pp} & U^{pe} \\ U^{ep} & U^{ee} \end{pmatrix} \begin{pmatrix} H^p \\ H^e \end{pmatrix} = \begin{pmatrix} C^p \\ C^e \end{pmatrix}. \tag{18}$$

Contrary to systems (14) and (15), which are ill-posed since the operator F is compact, the square system (18) is likely to be well-posed. In the following, we assume that both U and U^{pp} are nonsingular matrices, which will turn out to be true in our numerical experiments.

Remark : we can give a simple interpretation of each of the four blocks which compose the matrix of system (18). The block U^{pp} (resp. U^{pe}) corresponds to the propagating part of the scattering answers to the propagating incident modes (resp. evanescent incident modes), the block U^{ep} (resp. U^{ee}) to the evanescent part of the scattering answers to the propagating incident modes (resp. evanescent incident modes).

This is now a natural question to wonder if we shall restrict ourselves to the propagating modes, that is we solve $U^{pp}H^p = C^p$ rather than (18), or if we shall also use the evanescent ones. Indeed, only the propagating modes are still significant at long distance. Of course, this question is specific to the Linear Sampling Method in a waveguide. For sake of simplicity, we detail the analysis in the back-scattering situation. First, we define $s_0 = \sup_{x\in\mathcal{D}} x_1$. Without loss of generality, in this section the origin of axis x_1 is chosen such that $s_0 = 0$. With this convention, s is the distance between the obstacle and the section Σ_s where back-scattering measurements take place. With the help of lemma 1, we have that for all $n \geq 0$,

$$u_n^-(s, x_2) = \sum_{m\in\mathbb{N}} (u_n^-(0, x_2), \theta_m)_{\Sigma_0} e^{i\beta_m s}\theta_m(x_2),$$

and hence for all $m, n \geq 0$,

$$(U_n^-)_m^+ = (u_n^-(0, x_2), \theta_m)_{\Sigma_0}\, e^{i\beta_m s},$$

whence, given definition (17), for $0 \leq m, n \leq N-1$,

$$U_{mn} = e^{i\beta_m s} e^{i\beta_n s} U'_{mn}, \quad \text{with} \quad U'_{mn} := \frac{1}{i\beta_n}(u_n^-(0, x_2), \theta_m)_{\Sigma_0}.$$

We denote by K the diagonal $N \times N$ matrix which is formed by the $e^{i\beta_m s}$, and we decompose K into its propagating part K^p and its evanescent part K^e. Similarly, given definition (17),

$$C_m = e^{i\beta_m(s-z_1)} C'_m, \quad \text{with} \quad C'_m = \frac{1}{i\beta_m}\theta_m(z_2),$$

and we denote by $L = (L^p, L^e)$ the diagonal $N \times N$ matrix which is formed by the $e^{i\beta_m(s-z_1)}$. Using these definitions, the system (18) reads

$$\begin{pmatrix} K^p U'^{pp} K^p & K^p U'^{pe} K^e \\ K^e U'^{ep} K^p & K^e U'^{ee} K^e \end{pmatrix} \begin{pmatrix} H^p \\ H^e \end{pmatrix} = \begin{pmatrix} L^p C'^p \\ L^e C'^e \end{pmatrix}. \tag{19}$$

Remembering that in the matrices K^p and L^p, $\beta_m = \sqrt{k^2 - k_m^2} \in \mathbb{R}^+$ and that in the matrices K^e and L^e, $\beta_m := i\gamma_m$ with $\gamma_m = \sqrt{k_m^2 - k^2} \in \mathbb{R}^+$, for sufficiently large values of s the matrices K^e and L^e are small matrices compared to matrices K^p and L^p. In order to highlight this fact, in (19) we separate small terms of order 1 from terms of order 0, which leads by denoting $V^{pe} = K^p U'^{pe}$ and $V^{ep} = U'^{ep} K^p$, to

$$\begin{pmatrix} U^{pp} & V^{pe} K^e \\ K^e V^{ep} & K^e U'^{ee} K^e \end{pmatrix} \begin{pmatrix} H^p \\ H^e \end{pmatrix} = \begin{pmatrix} C^p \\ L^e C'^e \end{pmatrix}. \tag{20}$$

In (20), the matrices K^e and L^e are of order 1, while the other matrices are of order 0. Thus, it is clear that the blocks of the system in which K^e and L^e appear almost vanish for high values of s, and hence the system (20) becomes strongly ill-conditioned. Therefore, unless the distance s between the obstacle and the support of data $\hat{\Sigma}$ is small, we will solve $U^{pp} H^p = C^p$ rather than $UH = C$, which means we will use only the propagating modes. It seems hard to obtain a quantitative and *a priori* criterion on s to decide if we shall use the evanescent modes or not. However, the influence of evanescent modes is analyzed in section 6 from a numerical point of view.

5.3. Tikhonov/Morozov regularization

In realistic situations, we handle noisy data $u_n^{\pm}$, and therefore the matrix U in system (16) is not known exactly. The available matrix is U^δ, which is contaminated by some noise of amplitude δ, so that $|||U^\delta - U||| \leq \delta$. Here, $|||.|||$ is the matrix norm induced by the standard euclidean norm $||.||$ in $\mathbb{R}^N$. Following [9],

(i) we replace the system $U^\delta H = C$ by the following regularized system in the sense of Tikhonov

$$(U^{\delta *} U^\delta + \alpha I_N) H_\alpha = U^{\delta *} C, \tag{21}$$

(ii) the non negative parameter α is chosen following Morozov's strategy, i.e. as the unique solution of equation

$$\mu(\alpha) := ||U^\delta H_\alpha - C||^2 - \delta^2 ||H_\alpha||^2 = 0. \tag{22}$$

By using the singular value decomposition $\{\sigma_n; u_n, v_n\}$ $n = 0, ..., N-1$ of operator U^δ, we verify that

$$\mu(\alpha) = \sum_{n=0}^{N-1} \frac{\alpha^2 - \delta^2\sigma_n^2}{(\sigma_n^2 + \alpha)^2} |(C, v_n)|^2,$$

where $(.,.)$ is the standard scalar product of $\mathbb{R}^N$.
The reader will find a comprehensive analysis of the Tikhonov/Morozov regularization for compact operators in [8, 11].

Remark : when no noise is prescribed, which is a non realistic situation, we are not able to make a rigorous choice for parameter α in that case. Since U is nonsingular, we can simply put $\alpha = 0$ in (21), which exactly amounts to solve the system $U^\delta H = C$. This is a general fact that choosing $\alpha = 0$ in the Tikhonov regularization, which is of course not possible in the continuous case, is admissible in the discretized case since discretization induces regularization. As can be seen in the following section, the results are satisfactory for $\alpha = 0$ when no noise is prescribed, which indicates that in our case discretization provides enough regularization. Besides, these results are not significantly improved by a small α, which is anyway not possible to choose *a priori*.

6. Some numerical results

In our numerical experiments, we consider a 2D waveguide of height $h = 1$, and we perform the modal version of the Linear Sampling Method we described in the previous section, both in the full aperture and the back-scattering situations. In practice, we solve the Tikhonov system (21) with parameter α given by the Morozov's strategy in presence of noisy data (22) (and $\alpha = 0$ when no noise is prescribed), for each right hand side $C(z)$ of (16), when z takes all values of the sampling grid $[-t_0, t_0] \times [0, h]$, with $t_0 = \min(1, s)$. The figures hereafter represent the level curves of function $\log(1/||H_\alpha(z)||)$, so that the retrieved obstacle is the set of points z for which this function does not vanish.
We have tested two different obstacles :

(i) the obstacle is a sphere centered at $(0, 0.6)$ and of radius 0.2,

(ii) the obstacle consists of two spheres, the first one is centered at $(-0.2, 0.7)$ and is of radius 0.05, while the second one is centered at $(0.3, 0.5)$ and is of radius 0.07.

The synthetic data $u_n^\pm$ on $\hat{\Sigma} = \Sigma_{-s} \cup \Sigma_s$ (resp. $= \Sigma_s$) in the full aperture situation (resp. back-scattering situation) are obtained by introducing a weak formulation of problem (3) and then using a classical finite element method. Precisely, we used $P2$ classical Lagrange triangles based on a mesh which is sufficiently refined to be acceptable for the larger wavenumber k we consider in our numerical experiments. The Dirichlet-to-neumann condition on the artificial sections $\Sigma_{\pm t}$ requires the projection of the finite

element solution upon the transverse eigenfunctions θ_n, which diagonalize the Dirichlet-to-neumann operator.
In the following, in order to test the robustness of the method, we analyze how the quality of the reconstruction depends on some various parameters : the number of evanescent modes which are taken into account, the frequency and the amplitude of noise.

6.1. The influence of evanescent modes

In order to test the influence of evanescent modes, we consider two different positions for the support of data $\hat{\Sigma}$ following coordinate x_1: $s = 0.4$ and $s = 2$. In the following experiments, we consider the first obstacle (i) (one sphere) in the full aperture situation, and we take $k = 30$, which corresponds to a number $N_p = 10$ of propagating modes. Data are not corrupted by noise. A first computation using exactly the N_p propagating modes is considered as our reference case for both values $s = 0.4$ and $s = 2$, and we increase the total number of modes $N = N_p + N_e$ taken in the method, i.e. we use a number N_e of additional evanescent modes. The figure (1) shows the results of the reconstruction for $s = 0.4$ with respectively $N_e = 0$, $N_e = 5$, $N_e = 15$, $N_e = 25$, while the figure (2) shows the results of the reconstruction for $s = 2$ with respectively $N_e = 0$, $N_e = 1$, $N_e = 2$, $N_e = 3$.

We observe that for $s = 0.4$, using a few evanescent modes ($N_e \leq 5$) slightly improves

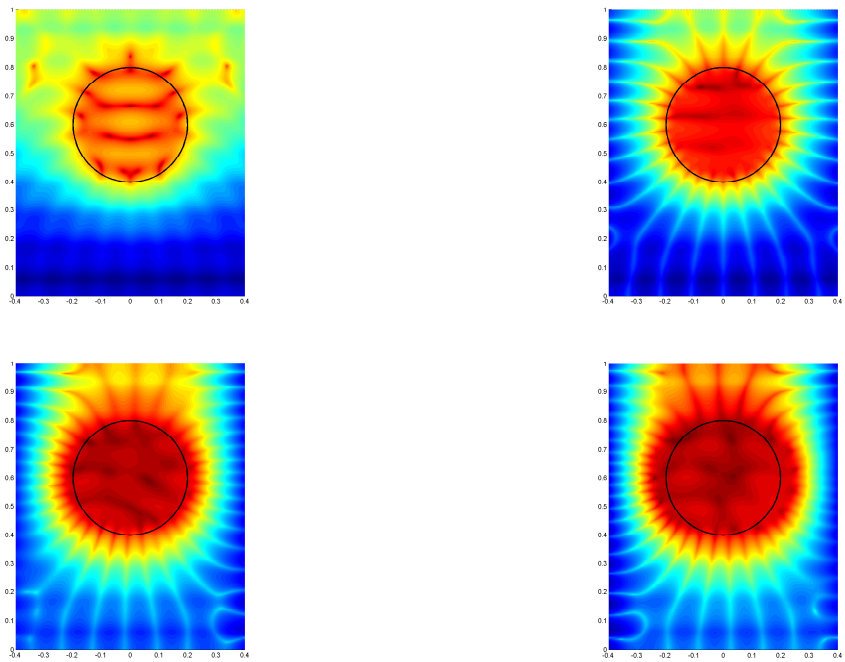

Figure 1. $s = 0.4$, $N_p = 10$, increasing values of N_e : $N_e = 0$ (top left), $N_e = 5$ (top right), $N_e = 10$ (bottom left), $N_e = 15$ (bottom right)

the reconstruction. If a larger number of evanescent modes is used, reconstruction

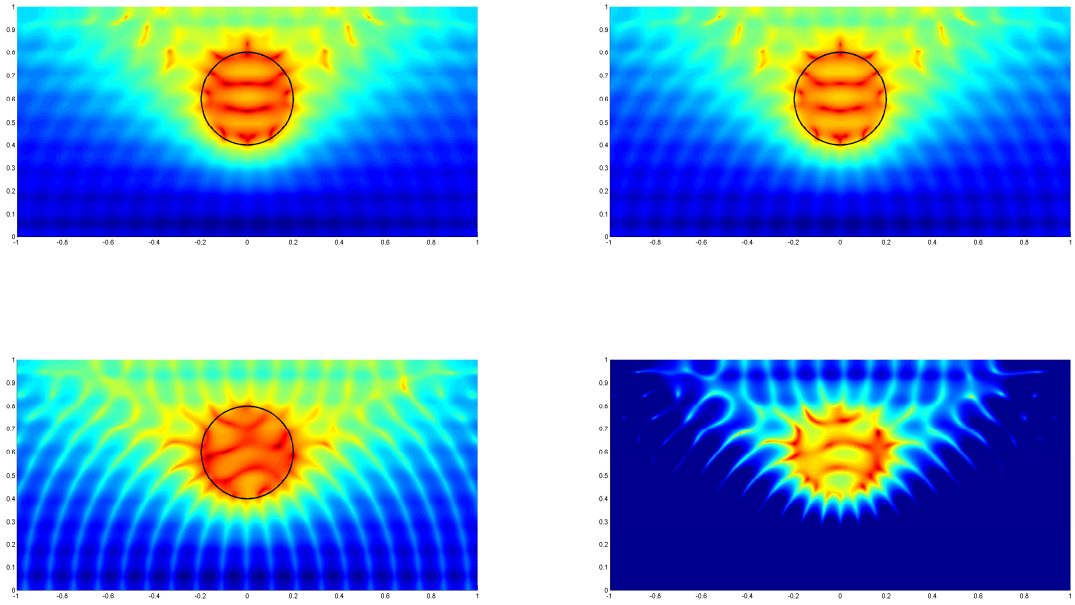

Figure 2. $s = 2$, $N_p = 10$, increasing values of N_e : $N_e = 0$ (top left), $N_e = 1$ (top right), $N_e = 2$ (bottom left), $N_e = 3$ (bottom right)

starts to deteriorate, and for $N_e > 20$, the condition number of matrix U is too large for inversion. Therefore, $s = 0.4$ could be considered as a near field situation. For $s = 2$, even a single evanescent mode ($N_e = 1$) hardly improves the reconstruction, which deteriorates as soon as $N_e > 1$, and for $N_e > 3$, the condition number of matrix U is too large for inversion. Therefore, $s = 2$ could be considered as a far field situation, for which only propagating modes shall be used. Since we are mainly interested in the far field situation, we consider the case $s = 2$ in the following.

6.2. The influence of frequency

We now test several wavenumbers $k = 10$, $k = 30$ and $k = 50$, the corresponding numbers of propagating modes being respectively $N_p = 4$, $N_p = 10$ and $N_p = 16$. In those experiments, we consider the first obstacle (i) and we take $s = 2$, which means that the support of data is sufficiently far away from the obstacle so that we can restrict ourselves to the propagating modes. Data are not corrupted by noise. The figure (3) shows the results of the reconstruction in the full aperture situation, while the figure (4) shows the same results in the back-scattering situation.

As expected, the quality is improved when we increase the number of propagating incident modes N_p, or equivalently when we increase the wavenumber k. Besides, reconstruction is logically better in the full aperture case than in the back-scattering case, particularly in the area of the obstacle which is not enlightened in the latter case.

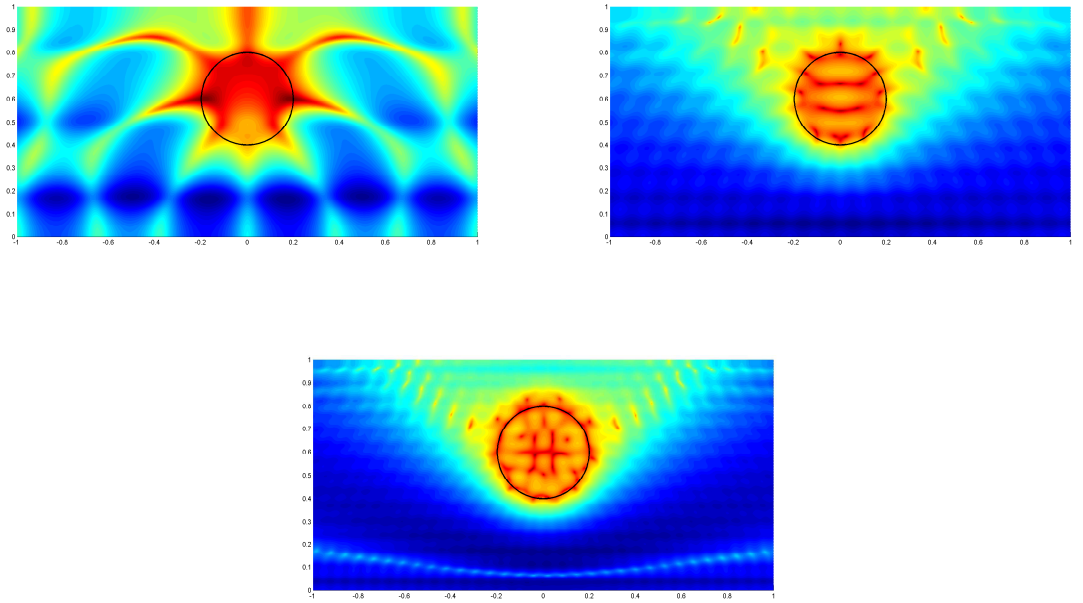

Figure 3. Full aperture, increasing values of k : $k = 10$, $N_p = 4$ (top left), $k = 30$, $N_p = 10$ (top right), $k = 50$, $N_p = 16$ (bottom)

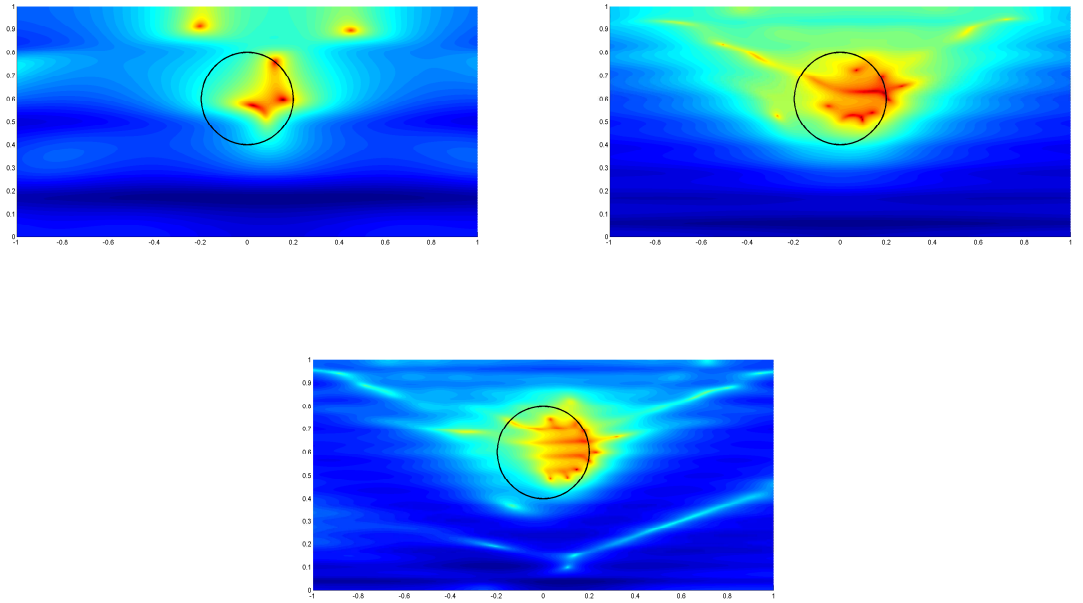

Figure 4. Back-scattering, increasing values of k : $k = 10$, $N_p = 4$ (top left), $k = 30$, $N_p = 10$ (top right), $k = 50$, $N_p = 16$ (bottom)

6.3. The influence of the amplitude of noise

The data $u_n^{\pm}$ obtained with our forward finite element computations are now subjected pointwise to a proportional Gaussian noise of various amplitude : 10% or 20%. We

present hereafter the impact of the amplitude of noise on the quality of the reconstruction of the second obstacle (*ii*) (two spheres) both in the full aperture situation and the back-scattering situation. Here, we have chosen $k = 30$ and $s = 2$. The figure (5) compares the uncorrupted and corrupted data u_0^- on Σ_s for the two levels of noise : 10% and 20%. The figure (6) shows the results of the reconstruction in the full aperture situation with the different amplitudes of noise, while the figure (7) shows the same results in the back-scattering situation.
We notice that the quality of the reconstruction is hardly affected by the error which contaminates the data. Again, reconstruction is much better in the full aperture case than in the back-scattering case.

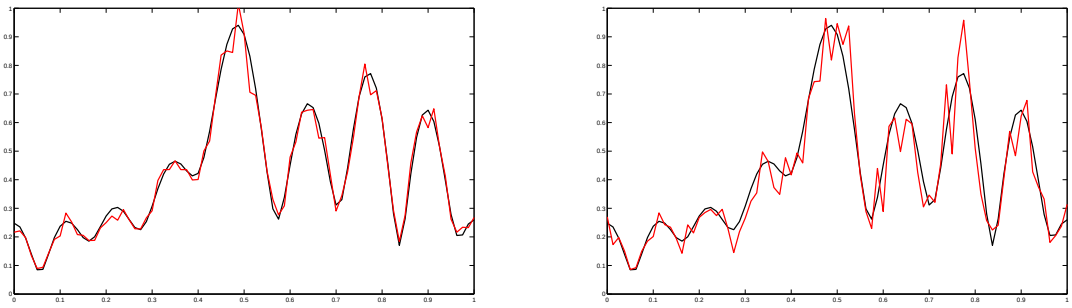

Figure 5. Black line : uncorrupted data. Red line : data with 10% noise (left) and 20% noise (right)

Appendix A. Proof of lemma 1

We first assume that $u \in H^1((s,t) \times \Sigma)$ is a solution to the problem. Since for fixed $x_1 > s$ we have $u(x_1, .) \in H^{1/2}(\Sigma) \subset L^2(\Sigma)$, and since the θ_n form an orthonormal basis of $L^2(\Sigma)$, there exists a decomposition

$$u(x_1, x_2) = \sum_{n\in\mathbb{N}} c_n(x_1)\theta_n(x_2).$$

By using the equation $(\Delta+k^2)u = 0$ we obtain that for all n, $c_n''+\beta_n^2\, c_n = 0$, which means that the $c_n(x_1)$ are linear combinations of $e^{i\beta_n x_1}$ and $e^{-i\beta_n x_1}$. By using the radiation condition we obtain that $c_n(x_1) = h_n e^{i\beta_n x_1}$, and then $h_n = (h, \theta_n)_{\Sigma_s} e^{-i\beta_n s}$ by using the boundary condition $u = h$ at Σ_s. Hence, we obtain the function

$$u(x_1, x_2) = \sum_{n\in\mathbb{N}} (h, \theta_n)_{\Sigma_s} e^{i\beta_n(x_1-s)}\theta_n(x_2).$$

Conversely, the above function is a solution to the problem. It remains to prove that for all $t > s$, $u \in H^1((s,t) \times \Sigma)$. A straightforward calculation leads to

$$||u||^2_{L^2((s,t)\times\Sigma)} = \sum_{n\in\mathbb{N}} |(h, \theta_n)_{\Sigma_s}|^2 \int_s^t |e^{i\beta_n(x_1-s)}|^2\, dx_1.$$

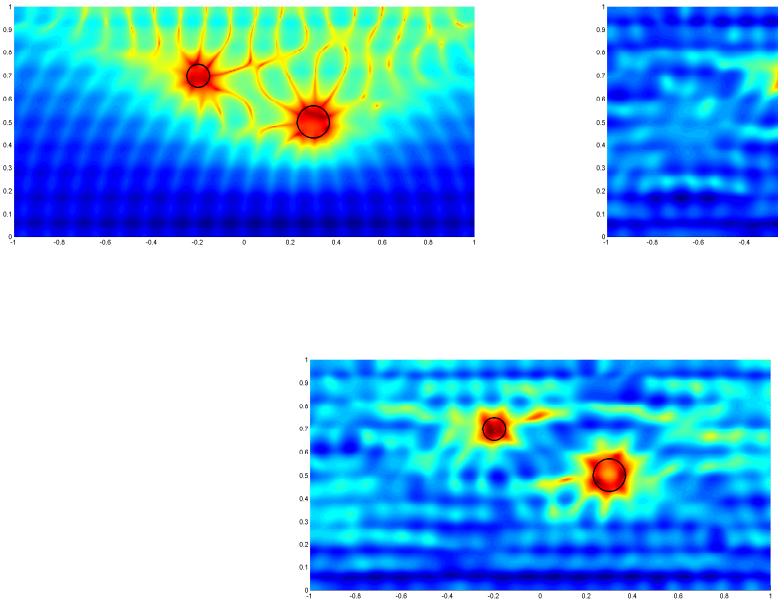

Figure 6. Full aperture, increasing noise : no noise (top left), 10% noise (top right), 20% noise (bottom)

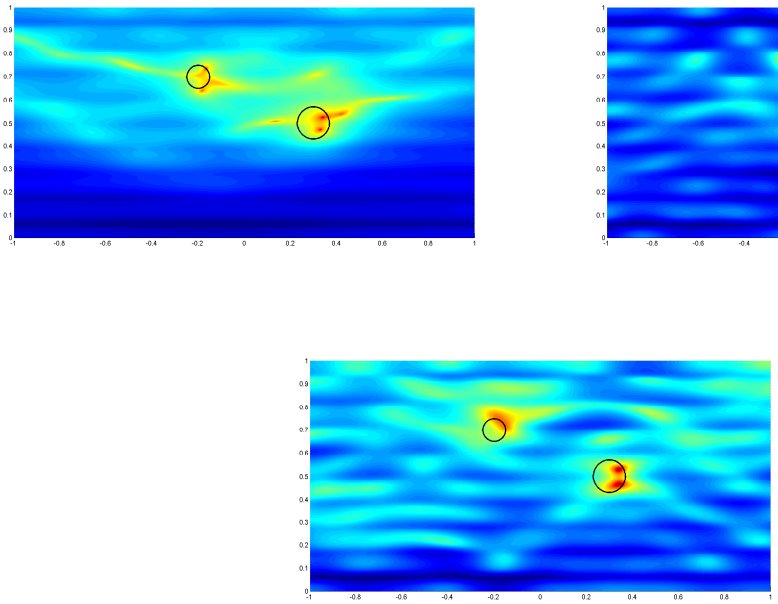

Figure 7. Back-scattering, increasing noise : no noise (top left), 10% noise (top right), 20% noise (bottom)

Here we have used the fact that $(\theta_m, \theta_n)_\Sigma = \delta_{mn}$. Besides,

$$\int_s^t |e^{i\beta_n(x_1-s)}|^2 \, dx_1 = \begin{cases} t-s & \text{if} \quad n < N_p \\ \frac{1}{2\gamma_n}(1-e^{-2\gamma_n(t-s)}) & \text{if} \quad n \geq N_p, \end{cases}$$

with $\gamma_n = \sqrt{k_n^2 - k^2}$ for $n \geq N_p$.
Moreover,

$$||\nabla u||^2_{L^2((s,t)\times\Sigma)} = ||\frac{\partial u}{\partial x_1}||^2_{L^2((s,t)\times\Sigma)} + ||\nabla_{x_2} u||^2_{L^2((s,t)\times\Sigma)}$$

$$= \sum_{n\in\mathbb{N}} |(h,\theta_n)_{\Sigma_s}|^2 (|\beta_n|^2 + k_n^2) \int_s^t |e^{i\beta_n(x_1-s)}|^2 \, dx_1.$$

Here we have used the fact that $(\nabla_{x_2}\theta_m, \nabla_{x_2}\theta_n)_\Sigma = k_n^2 \delta_{mn}$. As a result, we have

$$||u||^2_{H^1((s,t)\times\Sigma)} = \sum_{n\in\mathbb{N}} C_n |(h,\theta_n)_{\Sigma_s}|^2,$$

and C_n is equivalent to k_n when $n \to +\infty$.
Using a classical result of interpolation in Sobolev spaces, we have

$$H^{1/2}(\Sigma_s) = \{h = \sum_{n\in\mathbb{N}} h_n\theta_n, \quad \sum_{n\in\mathbb{N}} k_n |(h,\theta_n)_{\Sigma_s}|^2 < +\infty\},$$

which completes the proof.

Appendix B. Proof of lemma 2

The proof is inspired from [14]. We denote $\Omega = W \setminus \overline{\mathcal{D}}$. Let $x \in \Omega$ and $r > 0$ such that $B(x,2r) \in \Omega$ and g_x, $\tilde{g}_x$ the two functions defined by

$$\tilde{g}_x(y) = \begin{cases} 0 & y \in B(x,r) \\ -G(x,y) & y \notin B(x,r) \end{cases}$$

and

$$g_x(y) = G(x,y) + \tilde{g}_x(y).$$

Now we take $\psi \in C_0^\infty(\Omega)$, where $C_0^\infty(\Omega)$ denotes the set of infinitely differentiable functions which are compactly supported in Ω. As a distribution on Ω, $\tilde{g}_x$ satisfies

$$< (\Delta + k^2)\tilde{g}_x, \psi > = < \tilde{g}_x, (\Delta + k^2)\psi > = -\int_{\Omega\setminus B(x,r)} G(x,y)(\Delta + k^2)\psi(y) \, dy$$

$$= \int_{\Omega\setminus B(x,r)} \left(\psi(y)(\Delta_y + k^2)G(x,y) - G(x,y)(\Delta + k^2)\psi(y)\right) \, dy$$

$$= \int_{\partial B(x,r)} \left(\psi(y)\frac{\partial G(x,y)}{\partial \nu_y} - \frac{\partial \psi(y)}{\partial \nu_y} G(x,y)\right) \, ds(y),$$

where ν_y is the unit normal oriented inside $B(x,r)$, by using the Green formula. As a result,

$$< (\Delta + k^2)g_x, \psi > = \psi(x) + \int_{\partial B(x,r)} \left(\psi(y)\frac{\partial G(x,y)}{\partial \nu_y} - \frac{\partial \psi(y)}{\partial \nu_y} G(x,y)\right) \, ds(y).$$

The above relationship still holds for u instead of ψ. Indeed, if we take $\theta \in C_0^\infty(B(x,2r))$, with $\theta = 1$ on $\overline{B(x,r)}$, by using a classical result of regularity for elliptic problems,

$u \in C^\infty(B(x,2r))$ and hence the above equation is satisfied with $\psi := \theta u \in C_0^\infty(\Omega)$. The result follows from the fact that $\mathrm{supp}(g_x) \subset \overline{B(x,r)}$.
On the other hand,

$$< (\Delta + k^2) g_x, u >=< (\Delta + k^2) g_x, \theta u >=< g_x, (\Delta + k^2)(\theta u) >= 0,$$

which implies

$$u(x) + \int_{\partial B(x,r)} \left(u(y) \frac{\partial G(x,y)}{\partial \nu_y} - \frac{\partial u(y)}{\partial \nu_y} G(x,y) \right) ds(y) = 0. \tag{23}$$

Next, we use the Green formula in the subdomain Ω_t of $\Omega \setminus \overline{B(x,r)}$ which lies within sections Σ_{-t} and Σ_t.

$$\begin{aligned} 0 &= \int_{\Omega_t} \left(u(y)(\Delta_y + k^2) G(x,y) - G(x,y)(\Delta_y + k^2) u(y) \right) dy \\ &= \int_{\partial \mathcal{D}} \left(u(y) \frac{\partial G(x,y)}{\partial \nu_y} - \frac{\partial u}{\partial \nu_y} G(x,y) \right) ds(y) \\ &+ \int_{\partial B(x,r)} (.)\, ds(y) + \int_{\Gamma} (.)\, ds(y) + \int_{\Sigma_{-t} \cup \Sigma_t} (.)\, ds(y). \end{aligned}$$

The integral over $\partial \mathcal{D}$ has the sense of duality pairing between $H^{-1/2}(\partial \mathcal{D})$ and $H^{1/2}(\partial \mathcal{D})$. The integral over Γ vanishes because of the limit conditions satisfied by $G(.,y)$ and u. Now we consider the integral on Σ_t.

$$\int_{\Sigma_t} \left(u(y) \frac{\partial G(x,y)}{\partial \nu_y} - \frac{\partial u}{\partial \nu_y} G(x,y) \right) ds(y) = \int_{\Sigma_t} \left(u(y) T^+ G(x,y) - T^+ u(y) G(x,y) \right) ds(y).$$

Since for $h \in H^{1/2}(\Sigma_t)$, $h = \sum_n (h, \theta_n)\theta_n$ and $T^+ h = \sum_n i\beta_n (h, \theta_n)\theta_n$, we obtain that the above integral vanishes. Of course, the integral on Σ_{-t} vanishes as well. Thus we obtain that

$$\begin{aligned} &\int_{\partial B(x,r)} \left(u(y) \frac{\partial G(x,y)}{\partial \nu_y} - \frac{\partial u}{\partial \nu_y} G(x,y) \right) ds(y) \\ &\qquad = - \int_{\partial \mathcal{D}} \left(u(y) \frac{\partial G(x,y)}{\partial \nu_y} - \frac{\partial u}{\partial \nu_y} G(x,y) \right) ds(y). \end{aligned} \tag{24}$$

Gathering formulas (23) and (24), we obtain the announced result.

Appendix C. Proof of lemma 3

The proof is inspired from [8], p. 54. By using lemma 2, $u^s(.,y)$ has the representation

$$u^s(x,y) = \int_{\partial \mathcal{D}} \left(u^s(z,y) \frac{\partial G(x,z)}{\partial \nu_z} - \frac{\partial u^s(z,y)}{\partial \nu_z} G(x,z) \right) ds(z). \tag{25}$$

Interchanging the role of x and y gives

$$u^s(y,x) = \int_{\partial \mathcal{D}} \left(u^s(z,x) \frac{\partial G(y,z)}{\partial \nu_z} - \frac{\partial u^s(z,x)}{\partial \nu_z} G(y,z) \right) ds(z). \tag{26}$$

Besides, by using the Green formula, we obtain

$$0 = \int_{\partial\mathcal{D}} \left(G(x,z)\frac{\partial G(y,z)}{\partial \nu_z} - \frac{\partial G(x,z)}{\partial \nu_z} G(y,z) \right) ds(z) \tag{27}$$

and

$$0 = \int_{\partial\mathcal{D}} \left(u^s(z,x)\frac{\partial u^s(z,y)}{\partial \nu_z} - \frac{\partial u^s(z,x)}{\partial \nu_z} u^s(z,y) \right) ds(z). \tag{28}$$

We denote

$$\tilde{G}(.,y) = G(.,y) + u^s(.,y),$$

which is the Green function for the Helmholtz equation of the waveguide in presence of the soft obstacle $\mathcal{D}$. Adding (26) and (27), since $\tilde{G} = G + u^s$ and $G(x,y) = G(y,x)$ we obtain

$$u^s(y,x) = \int_{\partial\mathcal{D}} \left(\tilde{G}(z,x)\frac{\partial G(y,z)}{\partial \nu_z} - \frac{\partial \tilde{G}(z,x)}{\partial \nu_z} G(y,z) \right) ds(z). \tag{29}$$

Subtracting (28) to (25), we obtain

$$u^s(x,y) = \int_{\partial\mathcal{D}} \left(u^s(z,y)\frac{\partial \tilde{G}(z,x)}{\partial \nu_z} - \frac{\partial u^s(z,y)}{\partial \nu_z} \tilde{G}(z,x) \right) ds(z). \tag{30}$$

Finally, by subtracting (30) to (29), we obtain

$$u^s(y,x) - u^s(x,y) = \int_{\partial\mathcal{D}} \left(\tilde{G}(z,x)\frac{\partial \tilde{G}(z,y)}{\partial \nu_z} - \frac{\partial \tilde{G}(z,x)}{\partial \nu_z} \tilde{G}(z,y) \right) ds(z),$$

and hence $u^s(y,x) - u^s(x,y) = 0$ since $\tilde{G}(.,x)$ and $\tilde{G}(.,y)$ vanish on $\partial\mathcal{D}$.

Acknowledgements

The authors are indebted to the anonymous referees for their helpful remarks, in particular for improving the statement of theorem 2.

References

[1] T. Arens, A. Kirsch. The factorization method in inverse scattering from periodic structures. *Inverse Problems*, 19, 1195–1211, 2003.

[2] A.-S. Bonnet-Bendhia, F. Starling. Guided Waves by Electromagnetic Gratings and Non-uniqueness Examples for the Diffraction Problem. *Mathematical Methods in the Applied Sciences*, 17, 305–338, 1994.

[3] L. Bourgeois, C. Chambeyron, S. Kusiak. Locating an obstacle in a 3D finite depth ocean using the convex scattering support. *Journal of Computational and Applied Mathematics*, 204, 387–399, 2007.

[4] F. Cakoni, D. Colton. On the mathematical basis of the linear sampling method. *Georgian Mathematical Journal*, 10, 411–425, 2003.

[5] F. Cakoni, D. Colton. *Qualitative Methods in Inverse Scattering Theory*. Springer, 2006.

[6] D. Colton, J. Coyle, P. Monk. Recent Developments in Inverse Acoustic Scattering Theory. *SIAM Review*, 42(3), 369–414, 2000.

[7] D. Colton, A. Kirsch. A simple method for solving inverse scattering problems in the resonance region. *Inverse Problems*, 12, 383–393, 1996.
[8] D. Colton, R. Kress. *Inverse Acoustic and Electromagnetic Scattering Theory*. Springer, 1998.
[9] D. Colton, M. Piana, R. Potthast. A simple method using Morozov's discrepancy principle for solving inverse scattering problems. *Inverse Problems*, 13, 1477–1493, 1997.
[10] S. Dediu, J. R. Mc Laughlin. Recovering inhomogeneities in a waveguide using eigensystem decomposition. *Inverse Problems*, 22, 1227–1246, 2006.
[11] A. Kirsch. *An introduction to the Mathematical Theory of Inverse Problems*. Springer Verlag, 1996.
[12] A. Kirsch. Characterization of the shape of a scattering obstacle using the spectral data of the far field operator. *Inverse Problems*, 14, 1489–1512, 1998.
[13] R. Kress. *Linear Integral Equations*. Springer-Verlag, 1989.
[14] M. Lenoir. *Equations intégrales et problèmes de diffraction*. Cours de l'Ecole Nationale Supérieure des Techniques Avancées, 2005.
[15] R. Potthast. *Point sources and multipoles in inverse scattering theory*. Chapman & Hall/CRC, 2001.
[16] R. Potthast, J. Sylvester, S. Kusiak. A 'Range test' for determining scatterers with unknown physical proprieties. *Inverse Problems*, 19, 533–547, 2003.
[17] Y. Xu, C. Matawa, W. Lin. Generalized dual space indicator method for underwater imaging. *Inverse Problems*, 16, 1761–1776, 2000.